High-Magnetic Anisotropy of a Square-Planar Iron Carbene Complex

Brett M. Hakey,[a,#] Dylan C. Leary,[a,#] Jin Xiong,[b] Caleb F. Harris,[c] Jonathan M. Darmon,[d] Jeffrey L. Petersen,[a] John F. Berry,[c] Yisong Guo,[b]* and Carsten Milsmann[a]**

#B.M.H and D.C.L contributed equally.

[a]*C. Eugene Bennett Department of Chemistry, West Virginia University, Morgantown, West Virginia, USA.*

[b]*Department of Chemistry, Carnegie Mellon University, Pittsburgh, Pennsylvania, USA*

[c]*Department of Chemistry, University of Wisconsin-Madison, Madison, Wisconsin, USA.*

[d]*Department of Chemistry, Princeton University, Princeton, New Jersey, USA, 08544.*

camilsmann@mail.wvu.edu

ysguo@andrew.cmu.edu

berry_chem@wisc.edu

Supporting Information

Contents

1. X-Ray Crystallography

Single crystals suitable for X-ray diffraction were coated with polyisobutylene oil (Sigma-Aldrich) in a drybox, mounted on a nylon loop, and then quickly transferred to the goniometer head of a Bruker AXS D8 Venture fixed-chi X-ray diffractometer equipped with a Triumph monochromator, a Mo Kα radiation source (λ = 0.71073 Å), and a PHOTON 100 CMOS detector. The samples were cooled to 100 K with an Oxford Cryostream 700 system and optically aligned. The APEX3 software program (version 2016.9-0) was used for diffractometer control, preliminary frame scans, indexing, orientation matrix calculations, least-squares refinement of cell parameters, and the data collection. Three sets of 12 frames each were collected using the omega scan method with a 10 s exposure time. Integration of these frames followed by reflection indexing and least-squares refinement produced a crystal orientation matrix for the crystal lattice that was used for the structural analysis. The data collection strategy was optimized for completeness and redundancy using the Bruker COSMO software suite. The space group was identified, and the data were processed using the Bruker SAINT+ program and corrected for absorption using SADABS. The structures were solved using direct methods (SHELXS) completed by subsequent Fourier synthesis and refined by full-matrix least-squares procedures using the programs provided by SHELXL-2014.

Table S1. Crystallographic data for (^{Mes}PDP^{Ph})Fe(CPh_2)·C_7H_8.

	(^{Mes}PDP^{Ph})Fe(CPh_2)·C_7H_8
chem. formula	$C_{63}H_{55}FeN_3$
cryst size, mm^3	0.080 x 0.230 x 0.538
Fw, g mol^{-1}	909.95
space group	P $2_1/n$
a, Å	10.3547(6)
b, Å	15.2103(10)
c, Å	30.5374(18)
α, deg	90
β, deg	97.682(2)
γ, deg	90
V, Å	4766.4(5)
Z	4
T, K	100(2)
ρ calcd, g cm^{-3}	1.268
reflns collected/$2\Theta_{max}$	65302/54.98
unique reflns/I > 2σ(*I*)	10899/8893
No. of params/restraints	611/0
λ, Å	0.71073
R1[a]/goodness of fit[b]	0.0542/1.123
wR2[c] (*I* > 2σ(*I*))	0.1215
Residual density, e$Å^{-3}$	+1.325/-0.621

[a]Observation criterion: *I* > 2σ(*I*), $R_1 = \sum((||F_O| - |F_C||) / \sum|F_O|$. [b]GoF = $[\sum[w(F_o^2 - F_c^2)^2] / (n-p)]^{1/2}$. [c]$wR_2 = [\sum[w(F_o^2 - F_c^2)^2] / \sum[w(F_o^2)^2]]^{1/2}$

2. NMR Spectroscopic Data

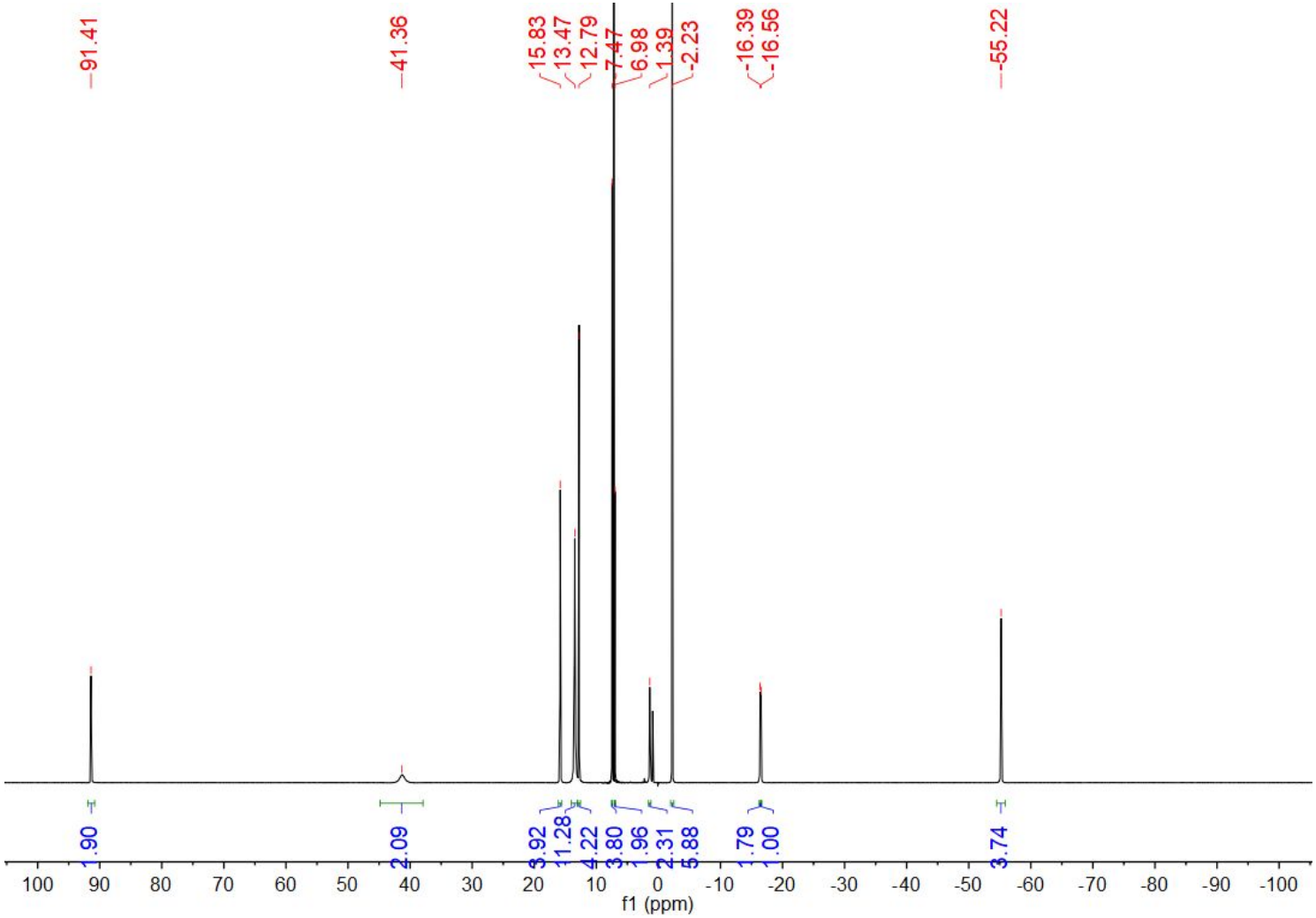

Figure S1. ^{1}H NMR spectrum (600 MHz) of (^{Mes}PDP^{Ph})Fe(CPh$_2$) in benzene-d_6 at room temperature.

3. ^{57}Fe Mössbauer Spectroscopy

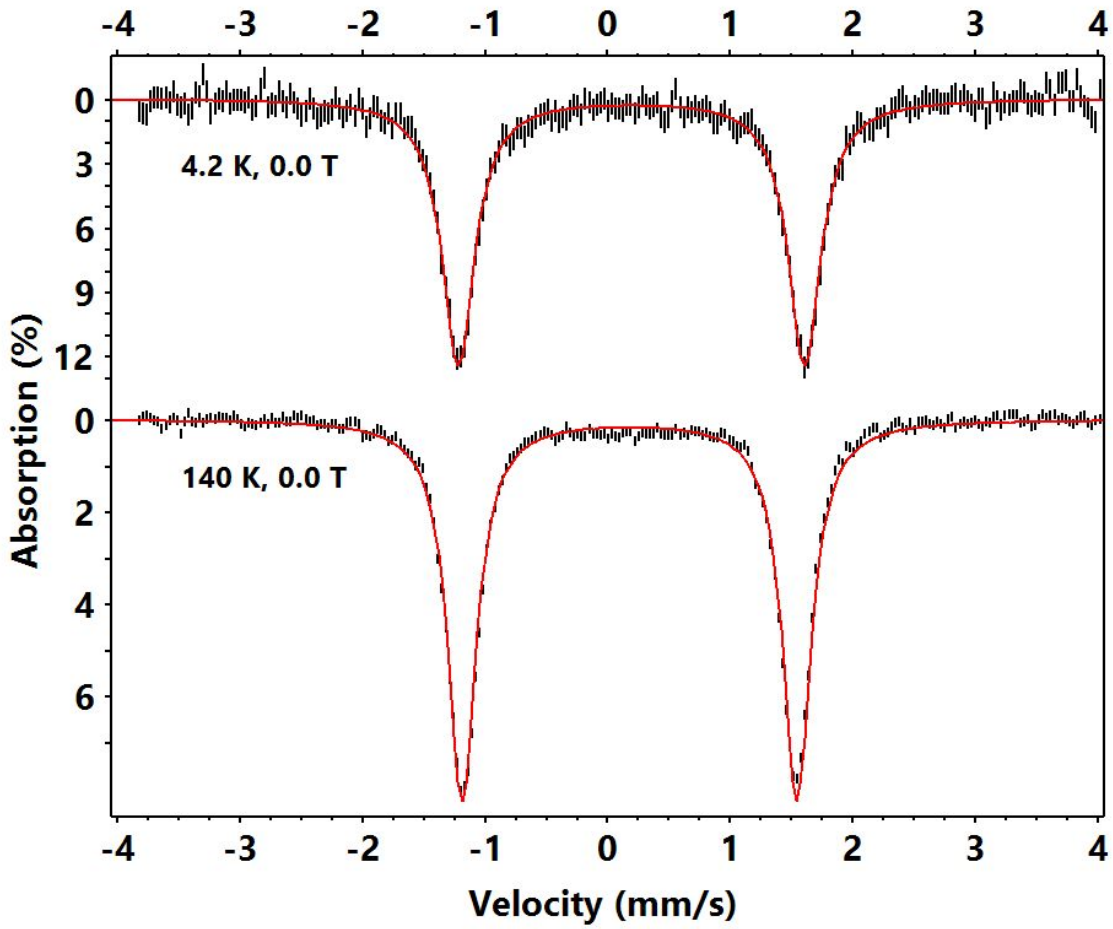

Figure S2. Zero-field Mössbauer spectra (black vertical bars) of a sample containing (^{Mes}PDP^{Ph})Fe(CPh_2) in solid powder form suspended in mineral oil at 4.2 K and 140 K. Red curves show corresponding simulations. The simulations give δ of 0.20 mm/s (4.2 K), 0.17 mm/s (140 K); $|\Delta E_Q|$ of 2.81 mm/s (4.2 K), 2.71 mm/s (140 K); Γ of 0.32 mm/s (4.2 K), 0.28 mm/s (140 K).

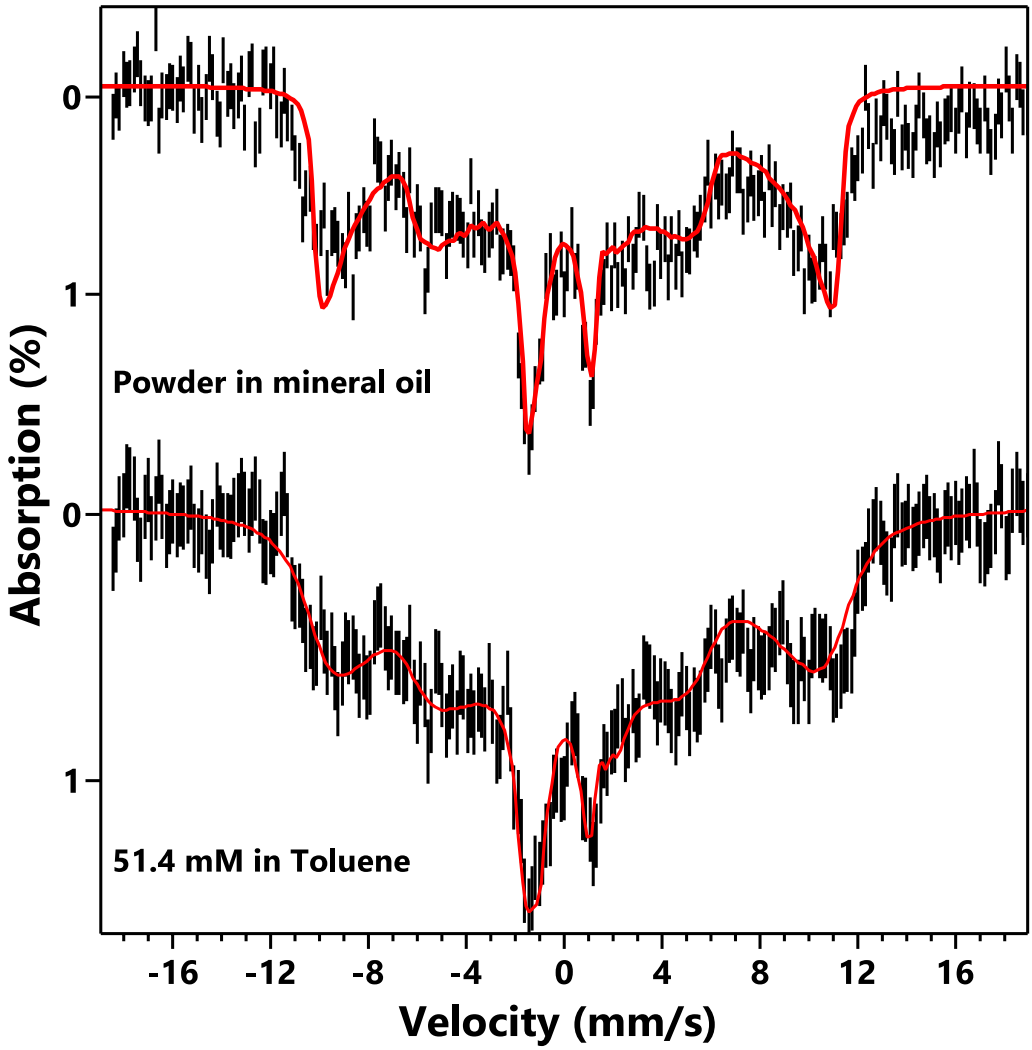

Figure S3. Mössbauer spectra under 4.2 K, 4.0 T of solid and solution samples of (^{Mes}PDP^{Ph})Fe(CPh$_2$). Red curves indicate simulations. Both spectra were simulated by using the same simulation parameters listed in the main text. For the solution sample, a wide distribution model on A_z is additionally employed (Lorentzian distribution). The center of A_z is set to + 73 T with a FWHM of 7.3 T (10%). A similar quality simulation could be obtained by including a distribution of the Rhombic zero field splitting parameter, E.

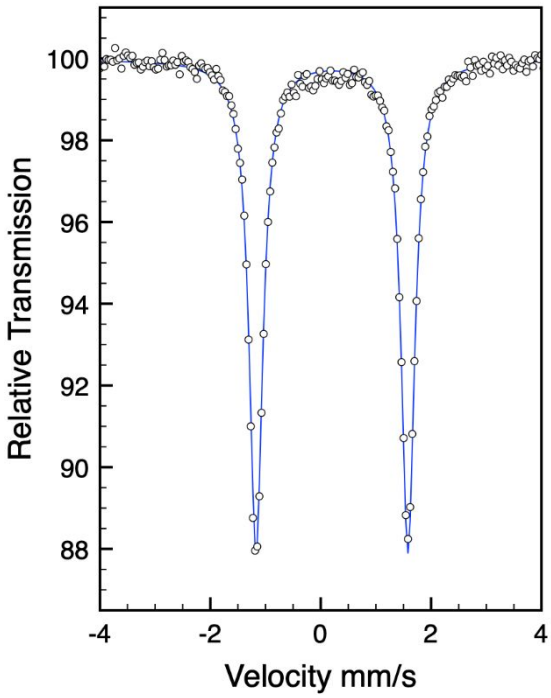

Figure S4. Zero-field ^{57}Fe Mössbauer spectrum of (^{Mes}PDP^{Ph})Fe(CPh$_2$) recorded at 80 K.

4. IR Spectra

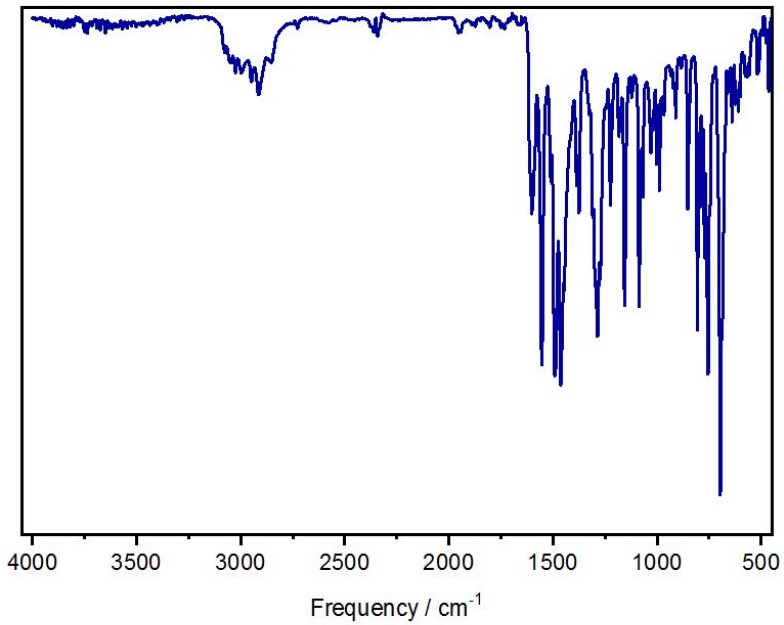

Figure S5. IR spectrum of (^{Mes}PDP^{Ph})Fe(CPh$_2$) (KBr).

5. Computational Studies

5.1 Additional Computational Data

Table S2. Comparison of DFT Methods on Optimized Structures.

Functional	Formalism	Fe-$C_{carbene}$ / Å	Fe-N(1) / Å	Fe-N(2) / Å	Fe-N(3) / Å
BP86	UKS3	1.818	1.922	1.956	1.918
	BS(3,1)[a]	-	-	-	-
TPSSh	UKS3	1.819	1.913	1.943	1.915
	BS(3,1)	1.819	1.913	1.942	1.915
B3LYP	UKS3	1.821	1.933	1.951	1.935
	BS(3,1)	1.821	1.933	1.951	1.935
Experiment		1.850(2)	1.958(2)	1.978(2)	1.946(2)
[a]Convergence issues were encountered.					

Table S3. Comparison of DFT Methods on Electronic Structure Metrics.

Functional	Formalism	Energy / E_h	$\langle S^2 \rangle$	Fe Spin Population	$C_{carbene}$ Spin Population	S_{UCOs}	d[a]
BP86	UKS3	-3599.426035	2.179	2.439833	-0.343407	0.92124	0.15
	UKS3[b]	-3599.415527	2.193	2.462850	-0.351797	0.91382	0.16
	BS(3,1)[c]	-	-	-	-	-	-
TPSSh	UKS3	-3599.273149	2.243	2.567138	-0.413879	0.88665	0.21
	UKS3 [b]	-3599.268271	2.289	2.593385	-0.420331	0.86457	0.25
	BS(3,1)	-3599.273141	2.243	2.567171	-0.413877	0.88666	0.21
B3LYP	UKS3	-3597.573975	2.282	2.558167	-0.399417	0.86747	0.25
	UKS3[b]	-3597.576988	2.328	2.583865	-0.411221	0.84423	0.29
	BS(3,1)	-3597.573974	2.282	2.558416	-0.399582	0.86739	0.25
[a]Diradical character calculated as 1-S_{UCOs}^2 according to Neese et. al. JACS 2003, 125, 10997-11005. [b]Results from a single-point calculation on the hydrogen-only optimized geometry. [c]Convergence issues were encountered which could not be rectified.							

Table S4. Comparison of Computational Method on the Fe-$C_{carbene}$ Bonding Description.[a]

Method	Fe Spin Population	$C_{carbene}$ Spin Population	d[b]
BP86	2.462850	-0.351797	0.16
TPSSh	2.593385	-0.420331	0.25
B3LYP	2.583865	-0.411221	0.29
CASSCF(8,12)/DKH/def2-TZVPP	2.364532	-0.315308	0.40
CASSCF(26,23)-ICE/def2-SVP	2.392585	-0.369785	0.39
CASSCF(16,15)-ICE/def2-SVP	2.462159	-0.413732	0.44

[a]All values are from single-point calculations on the hydrogen-only optimized geometry. [b]Diradical character calculated as 2*sqrt{wt[20]*wt[02]/(wt[20]+wt[02])} for CASSCF and 1 - S_{UCOs}^2 for DFT according to Neese et. al. JACS 2003, 125, 10997-11005 and Neese et. al. JACS 2018, 140, 9531−9544.

Table S5. Comparison of Computational Methods on Zero-Field Mössbauer Parameters.

Method[a]	ΔE_q / mm s^{-1}	δ / mm s^{-1} [b]	η
BP86	-3.843 (-3.094)	0.266 (0.152)	0.301 (0.147)
TPSSh	-2.947 (-2.596)	-0.006 (0.093)	0.366 (0.128)
B3LYP	-2.556 (-2.473)	-0.076 (0.091)	0.314 (0.149)
CASSCF	-2.843	- [c]	0.452
Experiment	-2.81	0.20	0.45

[a]Values for DFT methods in parentheses correspond to single-point calculations performed on the hydrogen-only optimized structure. [b]Fit using δ = α(ρ - C) + β. (BP86: α = -0.425, β = 7.916, C = 11810; TPSSh: α = -0.376, β = 4.130, C = 11810; B3LYP: α = -0.366, β = 2.852, C = 11810) according to ref. [1]. [c]No calibration data are available in the literature.

Table S6. Comparison of DFT Methods on the ZFS and g Tensor.

Method	Geometry Optimized			Hygrogen Optimized		
	$[g_{min}\ g_{mid}\ g_{max}]$	D	E/D	$[g_{min}\ g_{mid}\ g_{max}]$	D	E/D
BP86	2.02 2.06 2.11	13.7	0.03	2.01 2.08 2.11	10.5	0.03
TPSSh	2.01 2.06 2.08	27.6	0.14	2.01 2.06 2.08	-13.4	0.32
B3LYP	2.01 2.12 2.17	-10.5	0.14	2.01 2.12 2.16	14.4	0.22

Table S7. Effects of State-Averaging on the CASSCF/NEVPT2 Calculated Magnetic Properties.[a]

Number of Roots Included	[g_{min} g_{mid} g_{max}]	ZFS / cm^{-1}	E/D
3	[1.90 2.08 3.06]	-97	0.05
7	[1.91 2.08 3.06]	-94	0.04

[a]Calculated using effective Hamiltonian theory as outlined in the text. All quintet and singlet states were found to be >10,000 cm^{-1} above the ground triplet state. Inclusion of these high-energy states only eroded the description of the lowest three triplet states and therefore the quality of the calculations

Table S8. Configuration Summary of Roots Included in CASSCF/NEVPT2 State-Averaging Trials.

Root	Major CFG
0	$(\sigma)^2(\pi_{xy})^2(xz)^2(yz)^1(z^2)^1(\pi^*_{xy})^0(\sigma^*)^0$
1	$(\sigma)^2(\pi_{xy})^2(xz)^1(yz)^1(z^2)^2(\pi^*_{xy})^0(\sigma^*)^0$
2	$(\sigma)^2(\pi_{xy})^2(xz)^1(yz)^2(z^2)^1(\pi^*_{xy})^0(\sigma^*)^0$
3	$(\sigma)^2(\pi_{xy})^2(xz)^1(yz)^1(z^2)^1(\pi^*_{xy})^1(\sigma^*)^0$
4	$(\sigma)^2(\pi_{xy})^1(xz)^2(yz)^2(z^2)^1(\pi^*_{xy})^0(\sigma^*)^0$
5	$(\sigma)^2(\pi_{xy})^1(xz)^2(yz)^1(z^2)^1(\pi^*_{xy})^1(\sigma^*)^0$
6	$(\sigma)^2(\pi_{xy})^1(xz)^2(yz)^1(z^2)^2(\pi^*_{xy})^0(\sigma^*)^0$

Table S9. Natural orbital composition from the ground-state CASSCF(8,12) calculation.

Orbital	Löwdin Composition		N_{occ}
	Fe (d contribution)	$C_{carbene}$ (s and p)	
211	33.9 d_{z^2} + 61.5 d_{xz}	-	1.96955
212	33.5 $d_{x^2-y^2}$	5.5 s + 34.1 p_x	1.87125
213	72.2 d_{xy}	15.2 p_y	1.73775
214	96.1 d_{yz}	-	0.99909
215	59.2 d_{z^2} + 32.6 d_{xz}	-	0.99756
216	31.9 d_{xy}	42.2 p_y	0.25355
217	65.2 $d_{x^2-y^2}$	3.8 s + 14.7 p_x	0.13030

Table S10. Configuration interaction vector from the ground-state CASSCF(8,12) calculation.

CI Vector $(xz/z^2)(\sigma)(\pi_{xy})(yz)(z^2/xz)(\pi^*_{xy})(\sigma^*)\{5 \times 4d \text{ orbitals}\}$[a]	**Weight**
222110000000	0.75577
221111000000	0.07231
211111100000	0.05024
220112000000	0.04217
212110100000	0.01453
202110200000	0.01029
210112100000	0.00670
201111200000	0.00544
200112200000	0.00455
121220000000	0.00401
[a]Note that the d_{xz} and d_{z^2} orbitals show some degree of mixing in the ground-state calculation which is absent in the state-averaged calculations.	

Table S11. Natural orbital composition from the SA-CASSCF(8,12) calculation.

Orbital	**Löwdin Composition**		$\mathbf{N_{occ}}$
	Fe (d contribution)	$C_{carbene}$ (s and p)	
211	33.3 $d_{x^2-y^2}$	5.4 s + 33.8 p_x	1.87717
212	72.9 d_{xy}	14.9 p_y	1.74270
213	92.3 d_{z^2}		1.32758
214	95.2 d_{xz}	-	1.32217
215	96.5 d_{yz}	-	1.31981
216	31.5 d_{xy}	42.3 p_y	0.24239
217	65.2 $d_{x^2-y^2}$	3.7 s + 14.3 p_x	0.12681

Table S12. Configuration interaction vectors from the SA-CASSCF(8,12) calculation with 3 triplets.

Root	**CASSCF Energy / cm^{-1}**	**CI Vector** $(\sigma)(\pi_{xy})(z^2)(xz)(yz)(\pi^*_{xy})(\sigma^*)\{5 \times 4d \text{ orbitals}\}$[a]	**Weight**
0	0	221210000000	0.42455
		222110000000	0.33334
		211211000000	0.03846
		212111000000	0.02881
		111211100000	0.02789
		201212000000	0.02263
		112111100000	0.02185
		202112000000	0.01678

		121210100000	0.00773
		212120000000	0.00712
		021210200000	0.00552
		122110100000	0.00537
		022110200000	0.00436
		101212100000	0.00358
		102112100000	0.00294
		011211200000	0.00288
1	647	222110000000	0.43596
		221210000000	0.32675
		212111000000	0.03729
		211211000000	0.02944
		112111100000	0.02841
		202112000000	0.02185
		111211100000	0.02139
		201212000000	0.01741
		122110100000	0.00686
		121210100000	0.00572
		022110200000	0.00561
		212120000000	0.00460
		021210200000	0.00422
		102112100000	0.00380
		101212100000	0.00272
		012111200000	0.00267
2	2393	221120000000	0.75506
		211121000000	0.06718
		111121100000	0.04719
		201122000000	0.04199
		212210000000	0.01551
		121120100000	0.01064
		021120200000	0.00932
		101122100000	0.00528
		011121200000	0.00493
		001122200000	0.00416

[a]Note that the d_{xz} and d_{z^2} orbitals show some degree of mixing in the ground-state calculation which is absent in the state-averaged calculations. Consequently, the configurational breakdown of the wavefunction *appears* different for the ground and first excited state between the two calculations.

Table S13. Spin-orbit coupled states from the SA-CASSCF/NEVPT2 calculation with 3 triplets.[a]

State	Energy / cm^{-1}	Root	Spin (M_S)	Weight	$P_{Boltzmann}$
0	0.00	0	1 (±1)	0.879	3.81e-01
		1	1 (±1)	0.118	
1	9.61	0	1 (±1)	0.871	3.64e-01
		1	1 (±1)	0.129	
2	101.35	0	1 (0)	0.991	2.34e-01
3	754.72	1	1 (0)	0.981	1.02e-02
4	849.18	1	1 (±1)	0.861	6.48e-03
		0	1 (±1)	0.110	
		2	1 (0)	0.029	
5	909.95	1	1 (±1)	0.871	4.85e-03
		0	1 (±1)	0.129	
6	2876.09	2	1 (±1)	0.992	3.89e-07
7	2910.72	2	1 (±1)	0.977	3.30e-07
		1	1 (0)	0.016	
8	2932.03	2	1 (0)	0.964	2.98e-07
		1	1 (±1)	0.021	

[a]The coordinate system was chosen to diagonalize the ZFS tensor according to Eff. Ham. theory.

Table S14. Approximate average natural orbital composition from the SA-CASSCF(8,12)/SORCI calculation (truncated model).

Orbital	Löwdin Composition		N_{occ}
	Fe (d contribution)	$C_{carbene}$ (s and p)	
107	32.7 $d_{x^2-y^2}$	6.3 s + 35.0 p_x	1.91648778
108	72.5 d_{xy}	16.1 p_y	1.82248962
109	87.4 d_{z^2}	-	1.32352812
110	90.1 d_{yz}	-	1.32307791
111	95.3 d_{xz}	-	1.32269896
112	32.6 d_{xy}	43.5 p_y	0.17360955
113	68.2 $d_{x^2-y^2}$	3.8 s + 13.6 p_x	0.08951585

Table S15. Configuration interaction vectors from the SA-CASSCF(8,12)/SORCI calculation with 3 triplets (truncated model).

State (ref. wt.)	SORCI Energy / cm^{-1}	CI Vector $(\sigma)(\pi_{xy})(z^2)(yz)(xz)(\pi^*_{xy})(\sigma^*)\{5 \times 4d \text{ orbitals}\}$	Weight
0 (0.9522)	0	222110000000	0.0113
		221210000000	0.0179
		221120000000	0.7796
		212210000000	0.0032
		211121000000	0.0332
		201122000000	0.0291
		121120100000	0.0064
		111121100000	0.0319
		021120200000	0.0058
1 (0.9521)	495	222110000000	0.6767
		221210000000	0.1185
		221120000000	0.0223
		212111000000	0.0265
		211211000000	0.0047
		202112000000	0.0229
		201212000000	0.0041
		122110100000	0.0047
		112111100000	0.0276
		111211100000	0.0048
		022110200000	0.0049
2 (0.9528)	1722	222110000000	0.1287
		221210000000	0.6750
		221120000000	0.0065
		212120000000	0.0035
		212111000000	0.0054
		211211000000	0.0293
		202112000000	0.0050
		201212000000	0.0268
		121210100000	0.0042
		112111100000	0.0052
		111211100000	0.0269
		021210200000	0.0048

Table S16. Orbital composition from a B3LYP single-point calculation on the hydrogen-only optimized geometry.

Orbital	Löwdin Composition[a]			
	Fe (d contribution)		$C_{carbene}$ (s and p)	
d_{z^2}/d_{xz}	48.9 d_{z^2} + 22.5 d_{xz}		-	
π d_{xy}	α	β	α	β
	87.9 d_{xy}	48.6 d_{xy}	1.9 p_y	22.9 p_y
d_{xz}/d_{z^2}	22.5 d_{z^2} + 66.2 d_{xz}		-	
d_{yz}	87.8 d_{yz}		-	
σ* $d_{x^2-y^2}$	38.2 $d_{x^2-y^2}$		0.8 s + 3.9 p_x	
[a]The magnetic orbital compositions are from the UCOs. QRO compositions were used for all others. The DKH-def2-TZVP basis set was used on all atoms in the first coordination sphere.				

5.2 Molecular Orbitals and Spin Density Plots

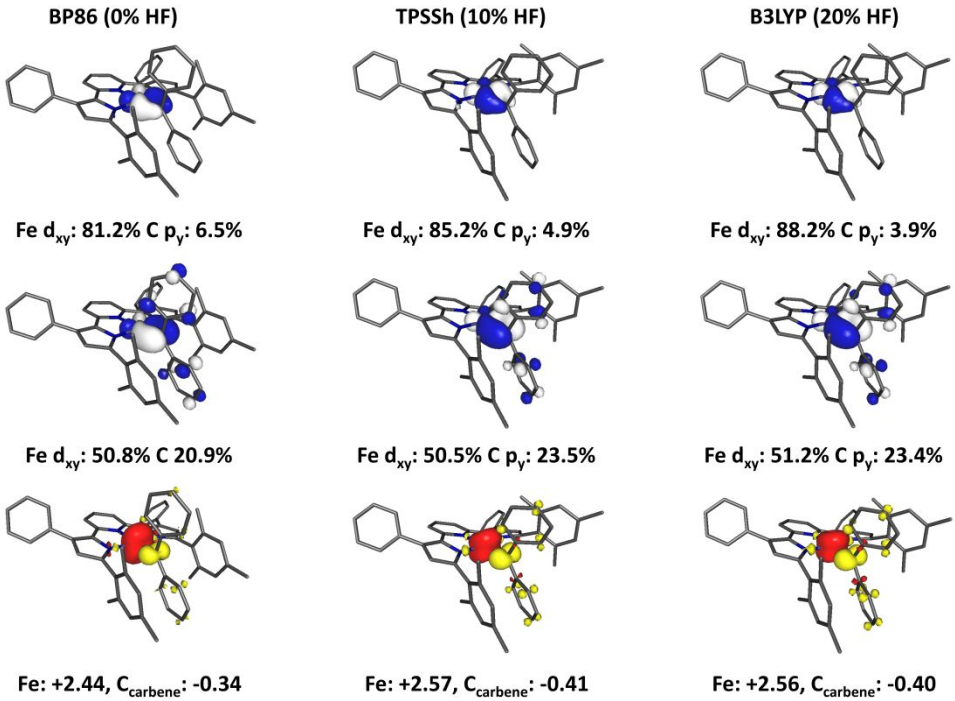

Figure S6. Corresponding orbitals (isovalue 0.04) and spin-density plots (isovalue 0.005) resulting from DFT calculations on the optimized geometries.

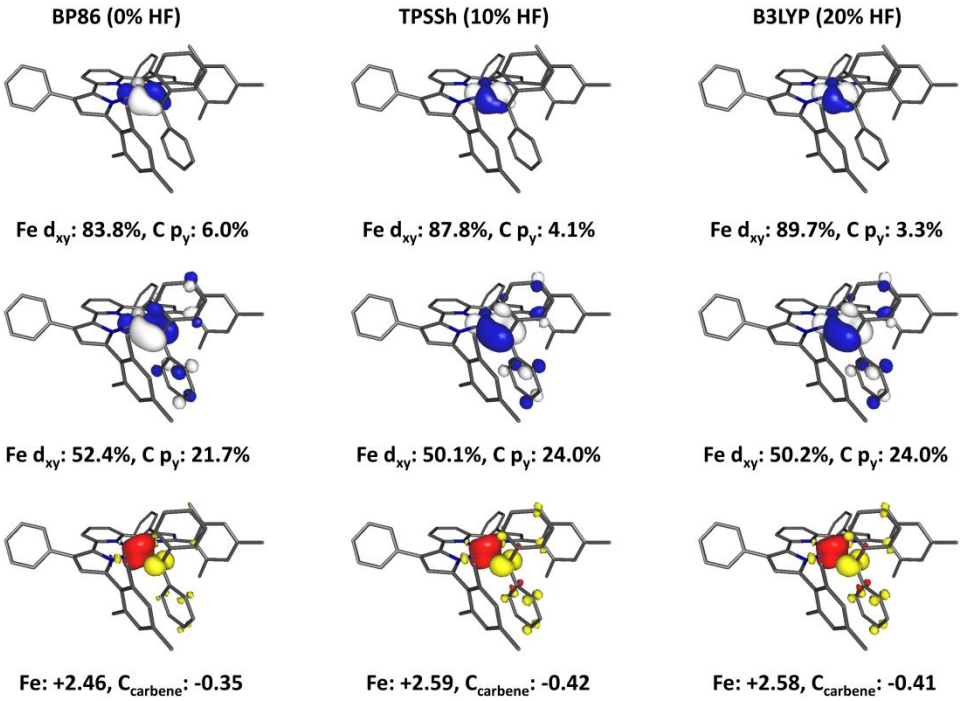

Figure S7. Corresponding orbitals (isovalue 0.04) and spin-density plots (isovalue 0.005) resulting from single-point DFT calculations on the hydrogen-only optimized geometry.

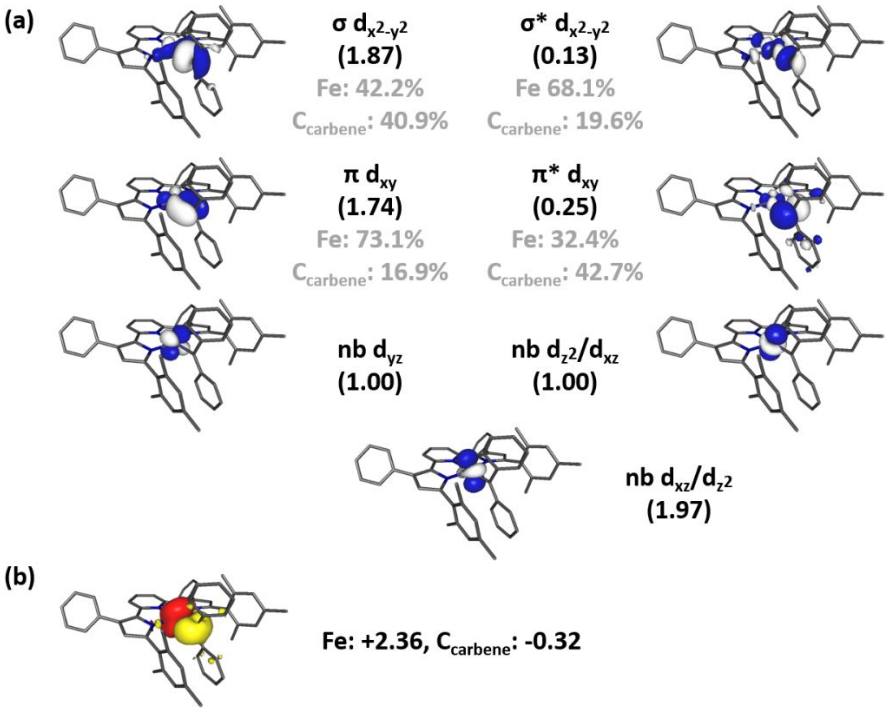

Figure S8. (a) Natural orbitals obtained from the ground-state CASSCF(8,12) calculation. The occupation numbers of the orbitals are shown below the orbital labels (nb = nonbonding) and atomic contributions to the molecular orbitals are shown in gray for the important orbitals. The double d-shell is omitted for clarity. (b) Mulliken spin density population obtained at the CASSCF(8,12) level.

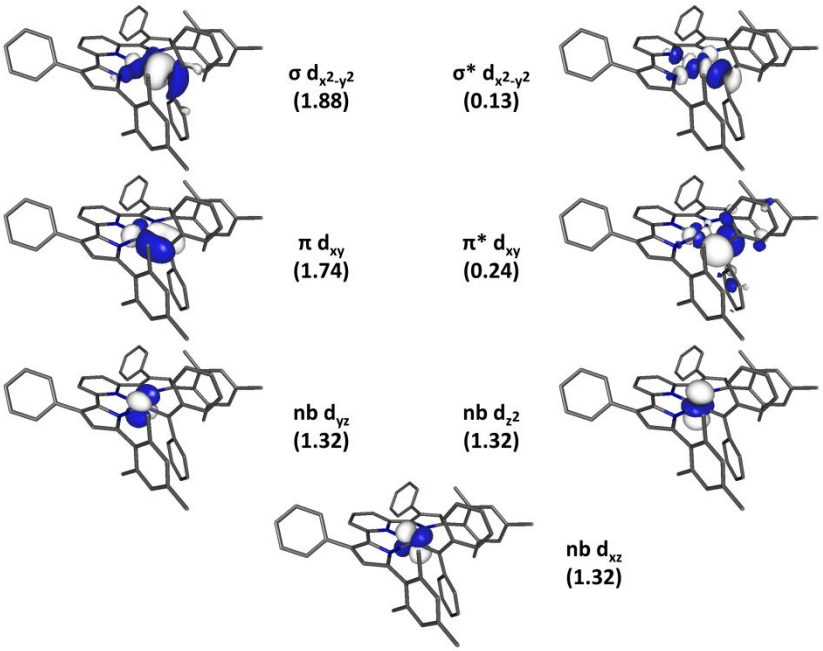

Figure S9. Natural orbitals (isovalue 0.04) of Fe(^{Mes}PDP^{Ph})(CPh_2) resulting from a SA-CASSCF(8,12) calculation (three triplets) at the DKH/def2-TZVPP level of theory. The occupation numbers are provided below the orbital assignment. The second d-subshell is excluded for clarity.

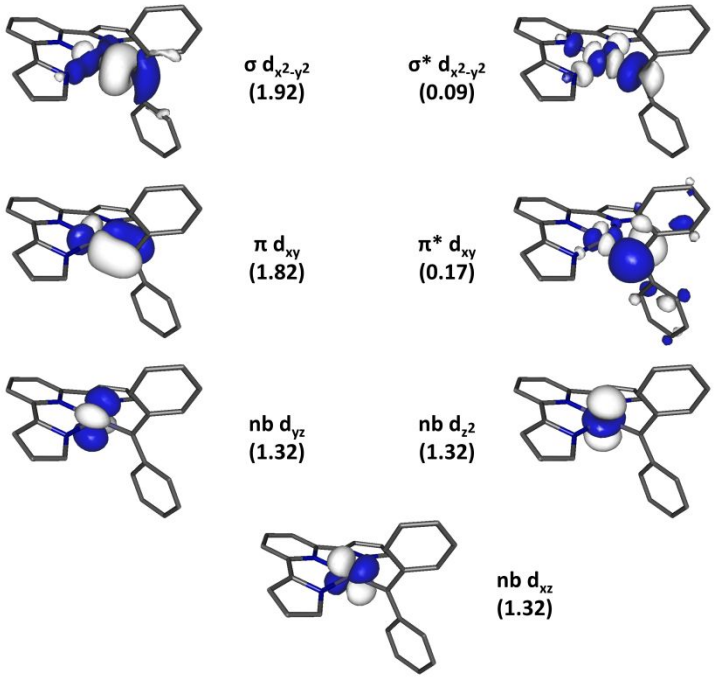

Figure S10. Approximate average natural orbitals (AANOs) (isovalue 0.04) of Fe(^{H}PDP^{H})(CPh_2) resulting from a SA-CASSCF(8,12)/SORCI calculation (three triplets) at the DKH/def2-TZVP(-f) level of theory. The occupation numbers are provided below the orbital assignment. The second d-subshell is excluded for clarity.

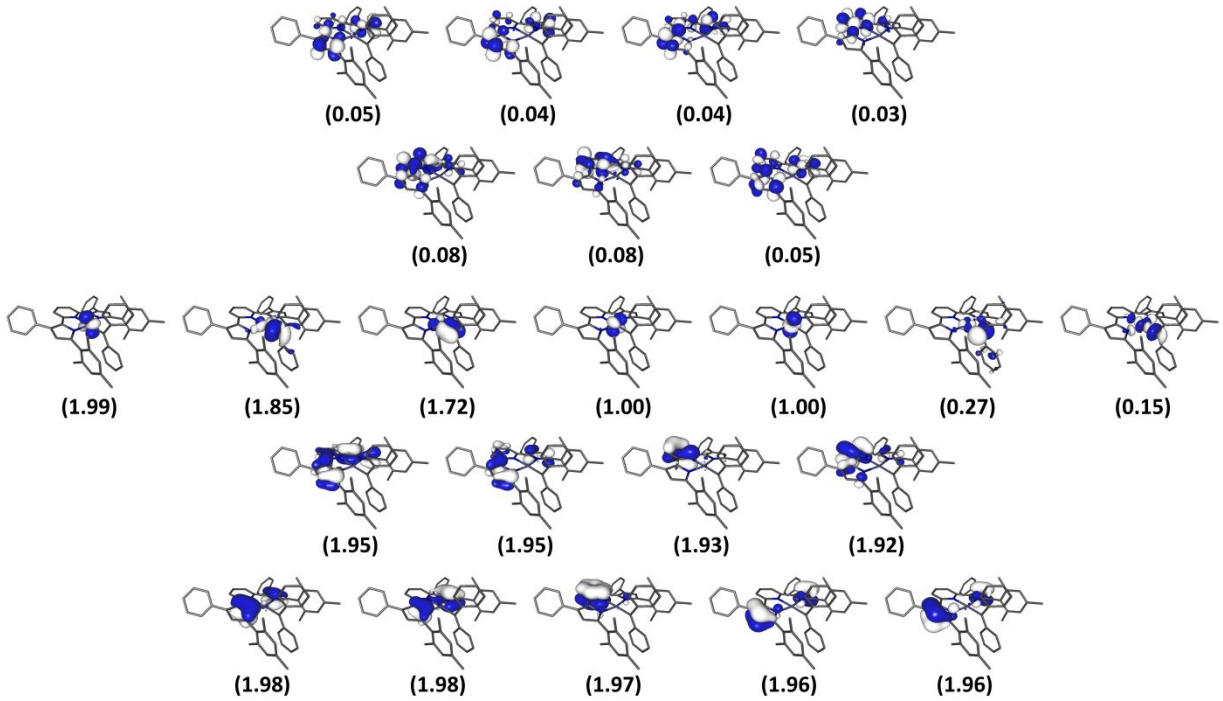

Figure S11. Natural orbitals (isovalue 0.04) of Fe(^{Mes}PDP^{Ph})(CPh_2) along with their occupation numbers resulting from a CASSCF(26,23)-ICE ground-state calculation at the def2-SVP level of theory. An appropriate approximation to the ligand active space could not be found despite numerous attempts.

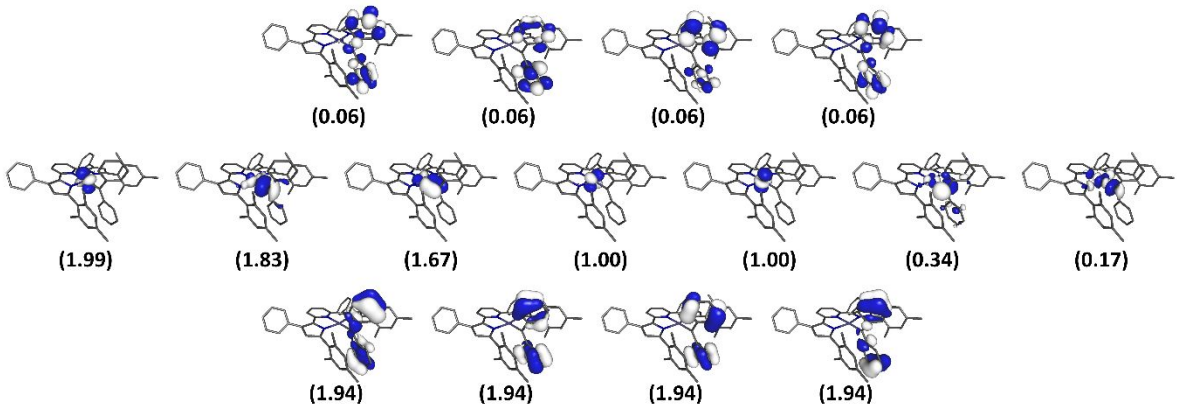

Figure S12. Natural orbitals (isovalue 0.04) of Fe(^{Mes}PDP^{Ph})(CPh_2) along with their occupation numbers resulting from a CASSCF(16,15)-ICE ground-state calculation at the def2-SVP level of theory. The CPh_2 π-system was approximated using 8 electrons in 8 orbitals.

5.3 Visualization of the Principle Components of g, D, and EFG Tensors

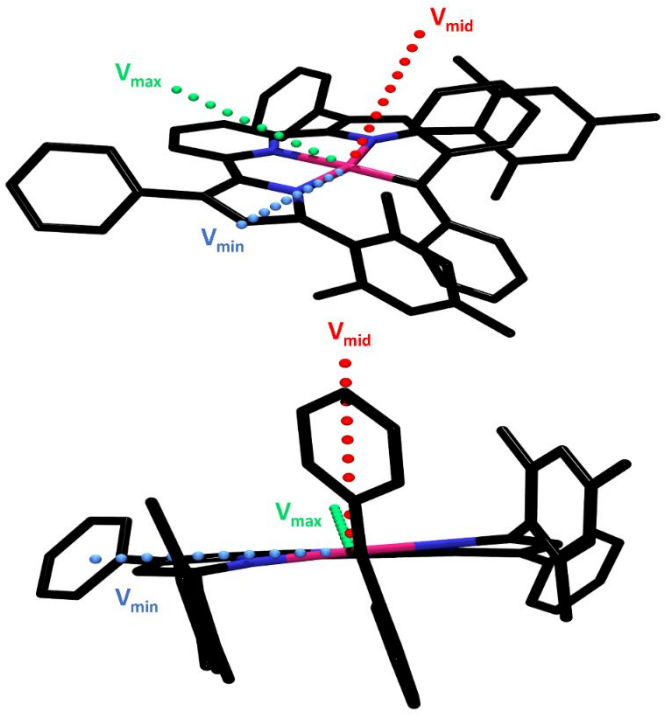

Figure S13. Principle components of the calculated electric field gradient resulting from a ground-state CASSCF(8,12) calculation.

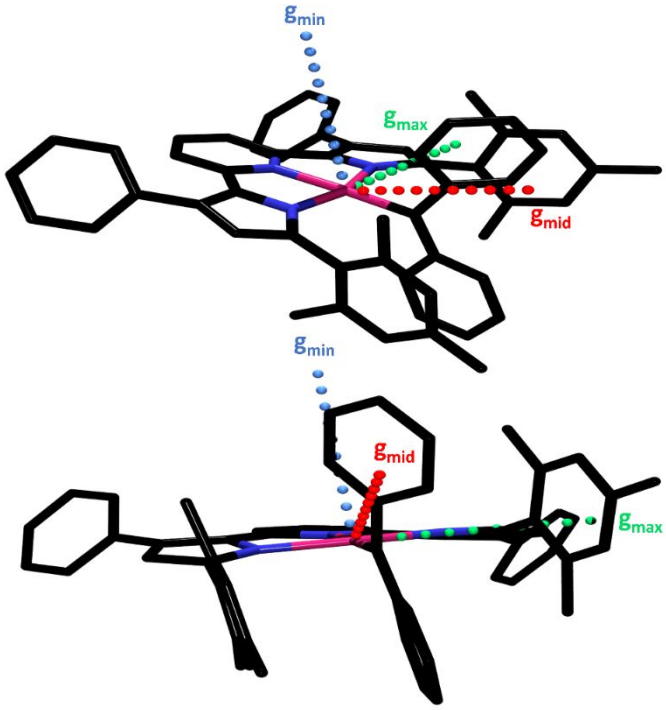

Figure S14. Principle components of the calculated g tensor resulting from a SA-CASSCF(8,12)/NEVPT2 calculation with three triplets.

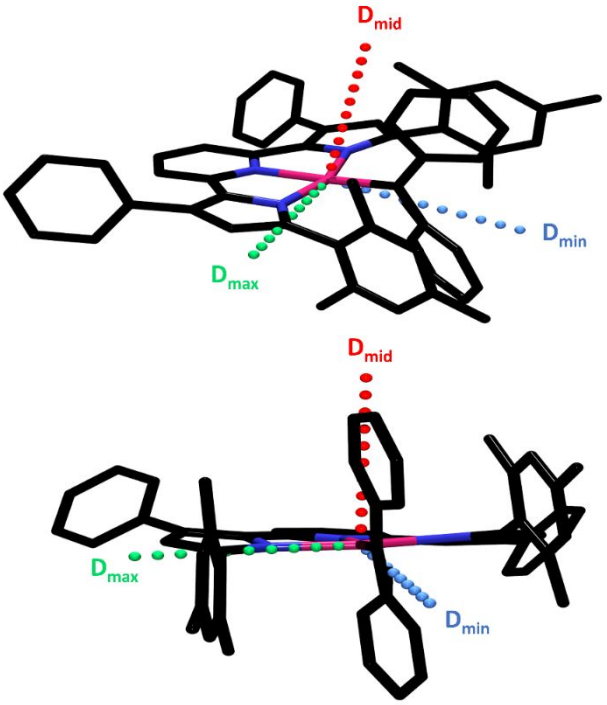

Figure S15. Principle components of the calculated ZFS resulting from a SA-CASSCF(8,12)/NEVPT2 calculation with three triplets.

5.4 Input Files

Input file for B3LYP geometry optimization

```
!uks b3lyp rijcosx tightscf slowconv dkh dkh-def2-svp autoaux normalprint uco uno tightopt
grid4 nofinalgrid gridx5 keepdens pal8
!d3bj
%basis newgto N "dkh-def2-tzvp" end end
%maxcore 4000
%scf MaxIter 500
  tole 1e-7
  tolerr 1e-6
  end
*xyz 0 3
Fe xyz coordinates          newgto "dkh-def2-tzvp" end
C_carbene xyz coordinates    newgto "dkh-def2-tzvp" end
.
.
*
```

Input file for hydrogen-only geometry optimization

```
!uks bp86 ri tightscf slowconv dkh dkh-def2-svp autoaux normalprint uco uno tightopt grid7
nofinalgrid keepdens
!d3bj
%basis newgto N "dkh-def2-tzvp" end end
%maxcore 4000
%pal nprocs 10
end
%geom optimizehydrogens true
end
%scf maxiter 500
  tole 1e-7
  tolerr 1e-6
  end
*xyz 0 3
Fe xyz coordinates newgto "dkh-def2-tzvp" end
C_carbene xyz coordinates newgto "dkh-def2-tzvp" end
.
.
*
```

Input file for DFT Mössbauer parameter calculation

```
!uks b3lyp nori tightscf slowconv def2-tzvp normalprint uco uno grid5 nofinalgrid keepdens
pal8
!kdiis soscf
%basis newgto N "def2-tzvp" end end
%method
  specialgridatoms 26
  specialgridintacc 7
end
%maxcore 4000
%scf maxiter 500
end
*xyz 0 3
Fe xyz coordinates newgto "cp(ppp)" end
C_carbene xyz coordinates newgto “def2-tzvp” end
.
.
*
%eprnmr nuclei = all Fe {rho, fgrad}
  End
```

Input file for DFT calculation of the ZFS and g tensor

```
!uks b3lyp rijcosx tightscf slowconv dkh dkh-def2-svp autoaux normalprint uco uno grid5 nofinalgrid gridx7 keepdens pal8
!kdiis soscf ri-somf(1x)
%basis newgto N "dkh-def2-tzvp" end end
%method
  specialgridatoms 26
  specialgridintacc 7
end
%rel
      picturechange 2
      finitenuc true
      fpfwtrafo false
end
%maxcore 4000
%scf maxiter 500
end
*xyz 0 3
   Fe xyz coordinates newgto "cp(ppp)" end
   C_carbene xyz coordinates newgto "dkh-def2-tzvp" end
.
.
*
%eprnmr gtensor true
       dtensor so
       dsoc cp
       ori      Fe xyz coordinates
  end
```

Input file for CASCI calculation to generate CASSCF starting orbitals

```
!dkh dkh-def2-svp rijcosx nofrozencore autoaux tightscf noiter
%maxcore 4000
%pal nprocs 8 end
%casscf nel 8
              norb 7
              mult 3
              nroots 1
              trafostep ri
              etol 1e-7
       end
*xyz 0 3
coords
*
```

Input file for CASSCF calculation of initial active space and second d-subshell preparation

```
!dkh dkh-def2-svp rijcosx nofrozencore autoaux tightscf moread
%moinp "dkhsvp-casci-orbitals.gbw"
%maxcore 4000
%pal nprocs 8 end
%scf rotate {orbital1,orbital2,90} end end    #rotation of the casci orbitals to give a proper active space
%casscf nel 8
        norb 7
        mult 3
        nroots 1
        trafostep ri
        etol 1e-7
        extorbs doubleshell
end
*xyz 0 3
coords
*
```

Input file for CASSCF calculation of final active space and Mössbauer calculation

```
!dkh dkh-def2-tzvpp rijcosx nofrozencore autoaux tightscf moread
%moinp "dkhsvp-cas87-gs-orbitals.gbw"
%maxcore 10000
%pal nprocs 4 end
%casscf nel 8
        norb 12
        mult 3
        nroots 1
        trafostep ri
        etol 1e-7
end
*xyz 0 3
coords
*
%eprnmr nuclei = all Fe {rho, fgrad}
  end
```

Input file for CASSCF/NEVPT2 calculation of magnetic properties

```
!dkh dkh-def2-tzvpp rijcosx nofrozencore dlpno-nevpt2 autoaux tightscf moread
%moinp "dkhtzvpp-cas812-gs-orbitals.gbw"
%maxcore 15000
%pal nprocs 12 end
%rel
    picturechange 2
    finitenuc true
    fpfwtrafo false
end
%casscf nel 8
            norb 12
            mult 3
            nroots 3
            trafostep ri
            etol 1e-7
            nevpt
              d3tpre 1e-13
              d4tpre 1e-13
            end
            rel
              printlevel 3
              dosoc true
              gtensor true
            end
      end
*xyz 0 3
coords
*
```

Input file for SORCI calculation of magnetic properties ($Fe^{H}PDP^{H}CPh_2$ model)

```
!dkh dkh-def2-tzvp(-f) autoaux nofrozencore tightscf moread
%moinp "dkhtzvp(-f)-cas812-3trip-orbitals.gbw"
%maxcore 20000
%pal nprocs 4 end
%rel
    picturechange 2
    finitenuc true
    fpfwtrafo false
end
%casscf nel 8
            norb 12
            mult 3
            nroots 3
            trafostep ri
            etol 1e-7
      end
%mrci
         citype sorci
         intmode ritrafo
         tsel 1e-6
         tpre 1e-5
         tnat 1e-5
         etol 1e-6
         rtol 1e-6
         allsingles false
         soc
           printlevel 3
           dosoc true
           gtensor true
         end
         newblock 3 *
         excitations cisd
         nroots 3
         refs cas(8,12) end
         end
end
*xyz 0 3
coords
*
```

Input file for CASSCF-ICE calculation

```
!def2-svp rijcosx def2/jk tightscf moread keepdens
%moinp "def2svp-cas87-gs-orbitals.gbw"
%maxcore 20000
%pal nprocs 8 end
%scf rotate {orbital1,orbital2,90} end end    #preparation of the occupied and virtual ligand π-orbitals
%casscf nel 26
        norb 23
        mult 3
        nroots 1
        trafostep ri
        etol 1e-7
        cistep ice
        ci
          tgen 1e-3
          maxiter 500
        end
end
*xyz 0 3
coords
*
```